Desorption Experiments on Organic Insulators with High Energy Particle Beams

By Per Håkansson
Division of Ion Physics, Department of Radiation Sciences
Uppsala University, Box 535, S-751 21 Uppsala, Sweden

Synopsis

Fast heavy ions can electronically sputter or cause desorption from many different kinds of insulating materials like water ice, condensed gases, alkali halide salts and organics. In this paper a summary of experiments on electronic sputtering of biomolecules with MeV energy particle beams will be given. Recent results on formation of 'buckyballs' when a certain polymer is irradiated with fast heavy ions will also be described.

1 Introduction

When an energetic particle hits a surface, atoms or molecules can be sputtered from the surface. In the case of slow heavy ions with keV energies a series of screened Coulomb collisions occurs, refered to as a collision cascade in the material. This can lead to ejection of surface atoms according to the established theory for nuclear elastic sputtering by Sigmund (1969). The sputtering yield is proportional to the nuclear elastic part of the stopping power of the primary ion. This means that above the maximum in the nuclear stopping power function, see figure 1, the sputtering yield will decreases with increasing primary ion energy, but it will always be present. This sputtering mechanism is effective in all materials.

Also fast heavy ions with MeV energies can cause sputtering. For conductors like metals the few data on total sputtering yields and the energy dependence of ion yields show that a large fraction of the particle yield is associated with nuclear elastic sputtering (see e.g. Wien, 1989). However, the energy spectra of some metal ions sputtered by fast heavy ions (Matthäus et al. 1993) as well as the high total Au yield sputtered from an Au foil with 1.3 GeV ^{238}U ions (Cheblukov et al. 1992) indicate that electronic excitations in the track of the incident particle contribute to sputtering even in metals.

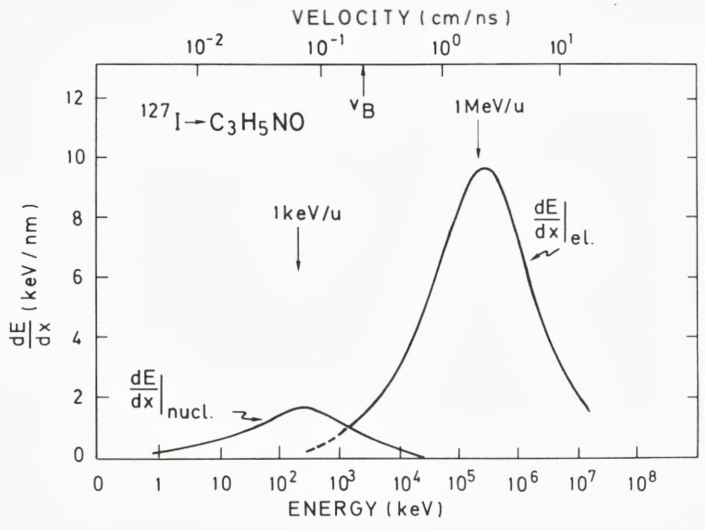

Figure 1. The nuclear and electronic stopping powers as a function of the primary ion energy (velocity). The values are for ^{127}I ions bombarding a target of C_3H_5NO. The Bohr velocity, $v_B = 0.22$ cm/ns, separates approximately the velocity regimes where, respectively, nuclear and electronic stopping dominate and thus also the two corresponding sputtering processes nuclear elastic sputtering and electronic sputtering.

In the case of many insulators, much higher sputtering yields have been measured for fast heavy ions than expected from nuclear elastic sputtering. As will be described in this paper, this new sputtering process in insulators is connected to the electronic part of the stopping power of the primary ion and is therefore called electronic sputtering to distinguish it from the nuclear sputtering process mentioned above. Fast heavy ions can sputter many different types of insulators (Wien, 1989), including water ice, metal oxides, condensed gases, alkali halide salts and biomolecules. Electronic sputtering is also called 'desorption' in the literature. Desorption and sputtering are often used interchangeably but 'desorption' generally applies to ejection of an adsorbed species, usually as an ion.

The Bohr velocity, $v_B = 0.22$ cm/ns, is the velocity of the electron in the hydrogen atom in Bohr's semiclassical atomic model. This velocity is often used to distinguish the two velocity regimes where either nuclear elastic stopping power or electronic stopping power dominates. Therefore it can also be used to roughly separate the corresponding processes, nuclear elastic sputtering from electronic sputtering, see figure 1. In this paper slow ions have a velocity $v < v_B$ whereas fast ions have $v > v_B$.

The fact that intact biomolecules can be sputtered as ions from a surface due to bombardment with fast heavy ions was discovered by Macfarlane and coworkers at Texas A&M University (Torgerson et al. 1974). Fission fragments from a radioactive source, ^{252}Cf, were used as primary ions. The electronic sputtering effect was exploited in an ion source using a new type of mass spectrometer in which the masses are determined by the time-of-flight technique. This form of mass spectrometry is called plasma desorption mass spectrometry, PDMS, by the inventors (Macfarlane & Torgerson, 1976). Both positive and negative ions can be analyzed. The remarkable finding is that large, non-volatile and thermally labile biomolecules, like peptides and proteins, can be studied with PDMS. The technique is now an important mass spectrometric tool for biological research of proteins (Sundqvist & Macfarlane, 1985; Roepstorff 1990). The largest observed molecular ions so far are from ovalbumin which has a molecular weight of 45 000 u (Jonsson et al. 1989). The important applications of electronic sputtering in the biosciences have over the years been a strong driving force in the attempts to elucidate the underlying physical desorption process.

1.1 Conversion of Energy into Molecular Motion

A central problem in electronic sputtering is to understand how the deposited energy can be converted to molecular motion which then leads to desorption (Johnson, 1987). How can a fast heavy ion, losing nearly 1 keV/Å in the target material, desorb intact proteins which are held together by rather weak bonds? The first suggested conversion mechanism was the Coulomb explosion of the positively charged infratrack (Haff, 1976). If the conductivity of the material is low enough there may be time enough to cause atomic and molecular motion due to the Coulomb repulsion before the track is neutralized. However, it has been claimed that even in insulators there may not be time enough for the Coulomb force to act due to the increased conductivity of the excited track core (Watson & Tombrello, 1985). Another possibility of the conversion of the deposited energy into atomic and molecular motion that has been suggested is excitation of the molecules to repulsive states with subsequent separation of the molecule (Johnson & Sundqvist, 1983; Watson & Tombrello, 1985). Furthermore, Williams & Sundqvist (1987) have suggested that an excitation to vibrational states by the flux of low-energy secondary electrons also will lead to larger separation between the molecules. The common idea with these mechanisms is that an expansion of the material will take place around the ion trajectory leading to molecular motion.

1.2 Desorption Mechanisms

Over the years many different desorption models have been proposed. To illustrate some different approaches to the problem a few models will be briefly described below. For more details the reader is referred to the review article in this volume by Reimann on desorption models. Common features for the described models below are the lack of an ionization mechanism and that a region around the point of impact of the primary ion is assumed to have too high energy density to allow desorption of intact molecules. From this region only molecular fragment and low-mass ions are assumed to be desorbed. However, recent experiments (see section 10) indicate that fullerenes can be formed in the central part of the ion track when a certain polymer is irradiated.

In the ion track model by Hedin et al. (1985) a statistical treatment is performed of the flux of secondary electrons that is generated by the primary ion when it is slowed down in the material (see section 3). These electrons propagate in the material and deposit energy when they are slowed down. The energy deposition at a certain point is approximately proportional to the flux of electrons at that point. In the model, which is a multihit model based on Poisson statistics, a molecule is desorbed if it is hit by a certain minimum number m of electrons. This is equivalent to requiring that a certain amount of energy must be deposited in the molecule for desorption to occur. The model can reproduce some general observations made by Håkansson et al. (1984) when the yield of large biomolecules is measured as a function of the electronic stopping power.

In the thermal model by Voit et al. (1989) the thermal flow is calculated to annular elements around the point of impact of the primary ion on the target surface from a number of sources of thermal energy along the trajectory of the primary ion. This energy is transferred from the kinetic energy of the primary ion through the electronic stopping power. The desorption probability is proportional to $\exp(-U_0/E_s)$ where U_0 is the surface binding energy and E_s the energy available at the molecular site. The yield is obtained by a summation over all time intervals, all sources and all annular elements weighted by the corresponding probability. The model is able to reproduce the dependence of measured secondary ion yields on the energy and initial charge state of the primary ions for light mass molecules like the amino acid valine (117 u).

In the continuum mechanical model or pressure pulse model by Johnson et al. (1989) the primary ion creates sources of impulses along its track through the solid. The energy from the individual sources spreads diffusively in the solid. In the case of a fast heavy ion with a large energy loss in the solid the sources act cooperatively and the energy density at any time is obtained by adding the contributions from the different sources. The resulting energy density gradient will cause a volume force

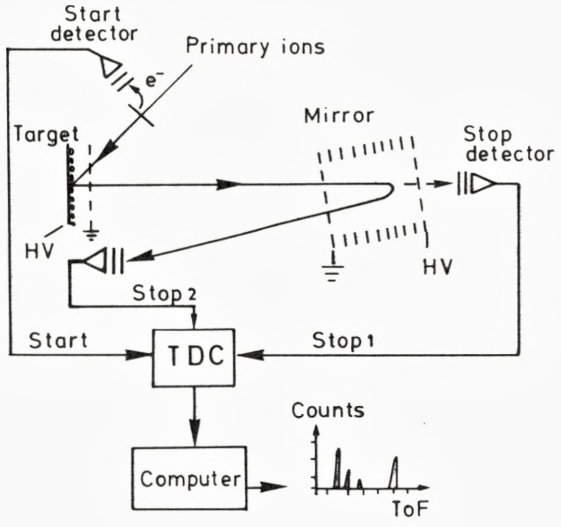

Figure 2. The principle of a time-of-flight, ToF, spectrometer with a single-stage mirror. Fast heavy ions from an accelerator (or fission fragments from a ^{252}Cf source) bombard the target on high voltage (HV). When the primary ions pass through a thin carbon foil in the start detector, a start signal for the ToF measurement is generated. The desorbed secondary ions are accelerated through a grid on earth potential into a field-free region. If the mirror voltage is off, the ions will continue into the straight stop detector and generate a stop signal. The time differences between the start and stop signals are converted into flight times by a time-to-digital converter, TDC. These are stored in a spectrum by a micro computer. With the mirror voltage on, only secondary ions will be reflected by the mirror into the second stop detector and no neutral decay products. This will improve the signal-to-noise ratio in the spectra. Furthermore, the mirror compensates for the initial axial velocity distributions of the ions and an improvement in time resolution and thus mass resolution will be obtained.

on the surrounding material, and by integrating this force over time the net impulse transferred to a volume element can be obtained. A molecule will be desorbed if the z-component of this impulse is larger than a critical impulse determined by the cohesive energy of the material. For a molecule on the surface one can show that the ejection will be at a certain angle relative to the nuclear track. The same directional ejection can also be obtained from a similar shock wave model introduced by Bitensky & Parilis (1987). The principal differences between these models are the description of the energy transport and the criterion for ejection (Fenyö & Johnson, 1992).

It is always difficult to justify the validity of a certain model based on a fit to a particular subset of experimental data. However, as will be shown in this paper, some basic electronic sputtering experiments on large biomolecules can only be

explained by expansion models like the pressure pulse model (Johnson et al. 1989) and the modified shock wave model (Bitensky et al. 1991).

Wien (1989) has reviewed the field of electronic sputtering in general and from insulators (Wien, 1992). Sundqvist (1991) has reviewed desorption of organic molecules induced by particle impact. This summary paper covers mainly experiments of electronic sputtering from organic insulators.

2 Experimental Methods

Electronic sputtering of ions can conveniently be studied with the time-of-flight (ToF) technique. This has been described in detail elsewhere (Macfarlane & Torgerson, 1976; Le Beyec, 1989; Sundqvist, 1991), and therefore only some basic facts will be described here. A schematic drawing of a ToF spectrometer is shown in figure 2. The target, which usually is at a potential of 10 - 15 kV, is bombarded with fast heavy ions from an accelerator. The desorbed and ionized molecules are accelerated through a grid on earth potential into a field-free drift region where they finally are stopped in a pair of microchannel plates. There, a shower of secondary electrons is created that generate a stop signal for the ToF measurement. The start signal is usually generated from a shower of secondary electrons produced when the primary ion is passing a thin carbon foil before hitting the target.

A common spectrometer design (Torgerson et al. 1974) where fission fragments from a ^{252}Cf source are used to bombard the target is the following. In the spontaneous fission of a ^{252}Cf nuclei two, almost collinear, fragments are created. One is then used to desorb the molecules on the target while the other is used to give a start signal for the ToF measurement.

In terms of desorption yield there is no difference between fission fragments from a ^{252}Cf source and an accelerator beam of ^{127}I ions with an energy around 80 MeV. However, in contrast to the fission fragments, the accelerator beam is well defined in energy, type of ion, angle of incidence and charge state, a prerequisite in many experiments. The time difference between start and stop signals is measured with a time-to-digital converter (TDC) and stored in a spectrum where the time scale is proportional to the square-root of the mass divided by the charge state of the ion. The data are recorded in event-by-event mode, which means that for each primary ion giving a start signal the corresponding stop signals are recorded. Usually a primary ion desorbs several secondary ions per impact so the TDC must be able to handle several stops per start.

Sometimes biomolecular ions are metastable and decay in flight. If this happens in the field-free region in the spectrometer it will lead to a broadening of the ToF peak. One way to get rid of neutrals and other decay products and thus to

improve the signal- to-noise ratio in the spectrum is to reflect the secondary ions in an electrostatic mirror. This will also make sure that a certain experiment is performed with stable ions. The mirror will compensate for the initial axial velocity distribution of the secondary ions and thereby improve the time resolution, and hence the mass resolution in a ToF spectrum. This was first demonstarted by Mamyrin et al. (1973) with a two-stage, second order compensating, mirror.

Today, mirrors are frequently used by many groups, and several different designs and applications exist. Here only a few will be mentioned. Tang et al. (1988) have compared the performance of a single-stage and two-stage mirror in SIMS-measurements. Della-Negra et al. (1987b) have developed an axial symmetric system with an annular microchannel plate stop detector that also is a two-stage mirror (Brunelle et al. 1991). A gridless mirror has been developed by Walter et al. (1986) for laser multiphoton postionization work. Brinkmalm et al. (1992b) have analyzed large biomolecules in a PDMS instrument with a single-stage mirror.

One common technique for preparing a target for a desorption experiment is to electrospray the molecules onto a metallic backing (McNeal et al. 1979). In the case of peptides and proteins, the technique used today is to adsorb the molecules to a polymer backing, usually a film of electrosprayed nitrocellulose (Jonsson et al. 1986).

3 Basic Ion-Track Concepts

When the nuclear sputtering yield is measured as a function of the primary ion energy, it first passes a maximum but is thereafter a continuously decreasing function for increasing primary ion energy. This is because the yield follows the nuclear stopping power (Sigmund 1969), see figure 1. However, it was independently found at Erlangen (Dück et al. 1980) and Uppsala (Håkansson et al. 1981b) that the yield for organics desorbed by fast heavy ions increased with increasing primary ion energy. This is also the case for the electronic stopping power function in this energy range. We therefore deal with electronic sputtering. Fundamental for the understanding of electronic sputtering is the concept of an ion track, and therefore some basic concepts are described below.

The energy loss of a fast heavy ion penetrating an insulator with a velocity above the Bohr velocity is dominated by electronic excitations and ionizations. Very little energy goes into nuclear collisions, which play no significant role in desorption from insulators at these incident particle energies. Along the path of the ion a cylindrical region with intense ionizations and excitations is produced due to direct Coulomb interactions, see figure 3. This region is called the infratrack (Brandt & Ritchie, 1974), and its radius scales with the velocity of the primary ion

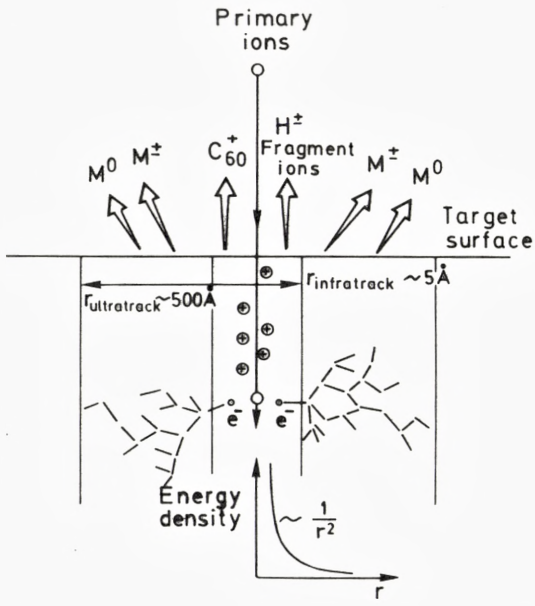

Figure 3. When a fast heavy ion passes through an organic target it will lose energy in a cylindrical region with intense ionizations and excitations due to direct Coulomb interactions. This region is called the infratrack and will become positively charged for a short time. The δ-electrons carry the excitation far out into the material and produce new generations of secondary electrons. This outer part of the track is called the ultratrack. The energy density of the deposited energy falls off like $1/r^2$ from the track centre. Light ions like H^+ and H^- are believed to be desorbed close to the track centre and so promptly that they feel the positively charged track core. Fragment ions are assumed to be created in the hot central part of the track region and desorbed closer to the track centre than molecular ions. Further out neutrals are desorbed. The molecular ions are desorbed with a strong directional correlation caused by the radially expanding track. In the case of a poly(vinylidene difluoride) target fullerenes are created in the hot central part of the track and ejected due to the axially expanding track.

(Sundqvist, 1993) :

$$r_{\text{infratrack}} \approx 6.7 \times (E/M)^{\frac{1}{2}} \text{ Å} \tag{1}$$

where E is the kinetic energy of the particle in MeV and M is the mass of the particle in u. Due to the direct interaction between the primary ion and target electrons, high energy δ-electrons are produced. These carry the excitation far out into the material and produce new generations of secondary electrons. This outer part of the track is called the ultratrack (Brandt & Ritchie, 1974). Its radius, which is determined by the projected range of the δ-electrons, scales as the square of the

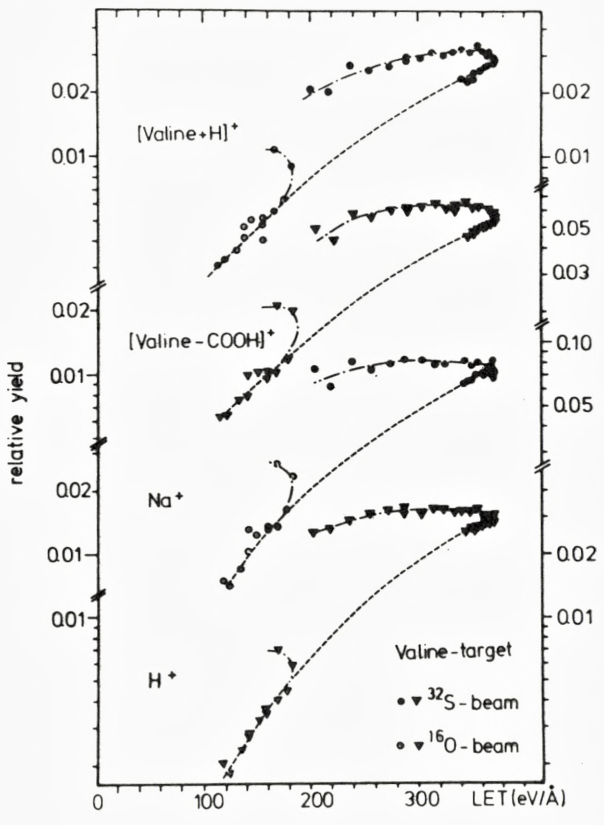

Figure 4. The yield of some different secondary ions from a valine target as a function of the linear energy transfer, LET, of the primary ions. (LET is the same as 'stopping power'). The target was bombarded with MeV energy ^{16}O ions (unfilled symbols to the left) and ^{32}S ions (filled symbols to the right). The same stopping power value can in certain cases be obtained with two different primary ion energies but the corresponding desorption yields are not necessarily the same. For each set of data points the lower branch corresponds to the high energy side and the upper branch to the low energy side of the stopping power function. The lines are guides for the eye, (Dück et al. 1980).

velocity of the primary ion (Sundqvist, 1993) :

$$r_{\text{ultratrack}} \approx 830 \times E/(\rho M)\text{Å} \tag{2}$$

Here ρ is the density of the material in g/cm^3. For 72 MeV ^{127}I ions, which is a typical fast heavy ion used in desorption experiments with biomolecules, these radii are approximately 5 and 500 Å respectively. The total energy loss per path length for such an ion is about 1 keV/Å and about 75 % (Kraft et al. 1992) of the deposited energy is converted into kinetic energy of the secondary electrons. The track zones are established within 10^{-15} s and the energy density falls off like $1/r^2$ (Kobetich & Katz, 1968) from the track centre.

4 Scaling of Yields with Electronic Stopping Power

In the literature, quite a lot of measurements can be found on how the yield of a certain biomolecular ion depends on the electronic stopping power of the primary ion. The data demonstrate the coupling of the sputtering process with the electronic rather than the nuclear part of the energy loss function. However, many of the yield vs. dE/dX curves exhibit a peculiar double-branch yield which make the interpretation of the data complex. This was shown already in the first accelerator experiments on electronic sputtering of biomolecules, namely valine desorbed by ^{16}O and ^{32}S beams by Dück et al. (1980), see figure 4.

The reason for the double branches is that the yield is a function of the deposited energy density in the track rather than a function of the total energy loss. When the primary particle energy is changed the track dimensions are also changed, as described in the previous paragraph. As a consequence the deposited energy per volume unit can decrease even if the total deposited energy increases. In a more well-defined experiment it is therefore important to keep the velocity of the primary ions constant, so the yield is measured as a function of the energy density rather than the electronic stopping power (Håkansson et al. 1984).

In the same paper Håkansson et al. also showed that when the yield of biomolecules is measured as a function of the electronic stopping power (energy density), the dependence on the stopping power will be steepest for low stopping power values and large molecules. This result has been confirmed both by Becker et al. (1986a) and Brandl et al. (1991). For large stopping power values the dependence will be approximately linear. There is also a threshold in energy density below which no molecular ions are observed. The larger the molecule the larger is this threshold. A 10 MeV ^{16}O beam will for example not desorb any molecular ions

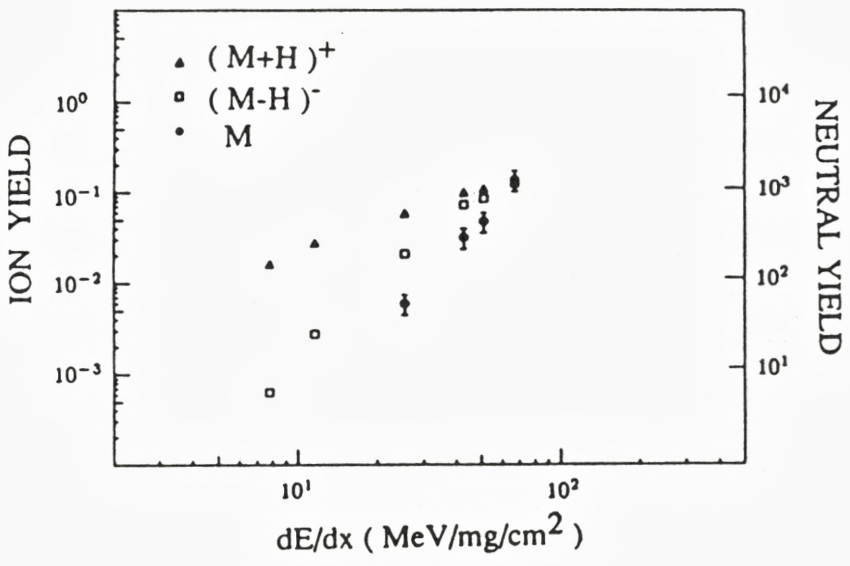

Figure 5. Absolute yields of intact neutral molecules (right scale) and normalized yields for positive and negative molecular ions (left scale) of the amino acid leucine as a function of the electronic stopping power of the primary ions. The energies of the different primary ions were chosen so the velocity was kept constant which means that the stopping power is proportional to the energy density in the ion track. The different scaling of the yields with energy density probably reflects different desorption mechanisms for neutrals vs. ions and indicates how far out from the track different species originate, (Hedin et al. 1987a).

from an electrosprayed target of insulin but it will produce a rather good spectrum of an amino acid (Hedin et al. 1987b).

There still exists only one complete set of data on the scaling of the yield for the neutral ejecta as well as the charged-particle ejecta with the electronic stopping power (energy density). That is for the amino acid leucine studied by Hedin et al. (1987a). The target was bombarded with beams of 20 MeV ^{32}S, 36 MeV ^{59}Ni, 49 MeV ^{79}Br and 78 MeV ^{127}I ions in charge-state equilibrium and with the same velocity for all the primary particles. The method used to measure the neutral yield will be described in the next section. The neutral yield was found roughly to follow a cubic dependence on the electronic stopping power (energy density). Including the primary ion beams 7 MeV ^{12}C and 10 MeV ^{16}O the scalings for positive and negative leucine molecules were found to be approximately linear and quadratic, respectively, as shown in figure 5. This is in agreement with recent results by Brandl et al. (1991) for the amino acid valine. The differences in scaling probably reflect different desorption mechanisms for neutrals vs. ions and indicate

how far out from the track different species originate (Johnson & Sundqvist 1992). Brandl et al. (1991) discuss the different scalings for positive and negative ions in terms of different ionization mechanisms.

5 Neutral-Yield Measurements

Because of the difficulties in measuring absolute total sputtering yields for biomolecular solids very few measurements are available. This is at present a problem in the comparison between experimental data and theoretical models, because so far most models contain no description of the ionization process.

In the two neutral yield measurements described in this paper the sputtered molecules were collected on clean pieces of silicon. To obtain the relative amount of material on the collector, it was rotated in the chamber to become a target in a small ToF spectrometer and analyzed with the PDMS technique. This was done in situ for the scaling experiment described above. To obtain the absolute amount of material on the collector, it was taken out from the chamber and analyzed with state-of-the-art amino acid analyzing technique.

The latter method was used by Salehpour et al. (1986) who irradiated a multilayer target of the amino acid leucine (131 u) with a beam of 90 MeV ^{127}I ions. Under the assumption of a $\cos\theta$ distribution for the sputtered molecules the yield of intact leucine molecules was found to be 1200 ± 200. The yield of positive ions of intact leucine molecules is only 13 % which gives a neutral-to-ion ratio of 10^4. With a molecular weight of 131 u and assuming a volume of 5×5×5 Å^3 for leucine the neutral yield corresponds to a total mass sputtered of nearly 160 000 u. This corresponds to a volume of a half sphere with a radius of 42 Å being removed (Sundqvist et al. 1989).

In a similar experiment with the collector method but performed under ultra high vacuum conditions, Nees (1988) has measured extremely high neutral yields from a testosterone hormone (274 u) and a derivate of it (428 u). The absolute yield of intact molecules sputtered by a 30 MeV $^{16}O^{5+}$ beam and determined with a biochemical method was found to be about 10^6 for both samples.

At present only these two measurements are available on the total sputtering yield, and it is not clear if the large difference in the numbers are an experimental fact or due to some artifacts. One can notice that the total yield in the pressure-pulse model (Johnson et al. 1989) is inversely proportional to the cohesive energy to the third power which could be very different for these two kinds of targets. This is consistent with the fact that refractory solids with large cohesive energies, like Al_2O_3, have very small total yields (Qiu et al. 1983). However, even with the lower value of the total sputtering yield for organics one can conclude that the total

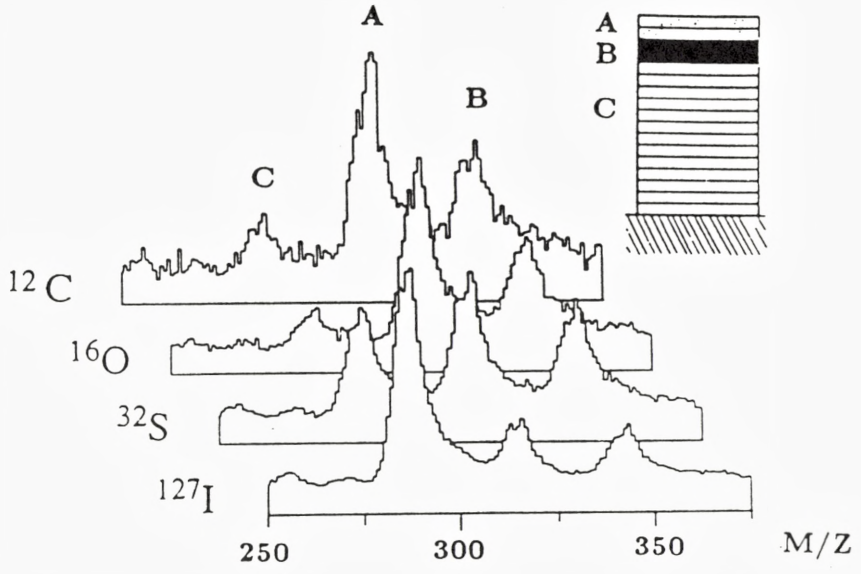

Figure 6. A Langmuir-Blodgett film was built up by 13 layers of stearic acid (C), 2 layers of behenic acid (B) and 2 layers of arachidic acid (A). Each layer had a thickness of 25 Å. The figure shows negative time-of-flight spectra around the molecular ion region for 4 different heavy ion beams. These have the same velocity which means that the corresponding stopping power values are proportional to the energy density in the ion track. The systematic change in the relative peak heights with energy density indicates crater formation. In the case of ^{127}I ions, secondary ions are observed from layers well below the surface indicating a sputtering depth of around 150 Å, (Säve et al. 1987a).

ejection is dominated by neutral molecules for these kinds of multilayer samples and molecules.

6 Electronic Sputtering from Langmuir-Blodgett Films

With the Langmuir-Blodgett technique it is possible to build targets of uniformly oriented organic molecules layer by layer. The films can be made very homogeneous and with well-defined thickness. The PDMS technique can be used to characterize the films, e.g. to discover incomplete salt formation or replacement of the original counter-ion by ions from the substrate surface (Schmidt et al. 1990). With spontaneous-desorption mass spectrometry (Della-Negra et al. 1985) defects in the

films, e.g. pinholes built in during the preparation, can be detected (Schmidt et al. 1991a).

Säve et al. (1987b) used such films to study the sample film thickness dependence in electronic sputtering and found that the yield saturates around 125 - 150 Å. By using different Cd-stabilized fatty acids with the only difference being the number of CH_2 groups in the hydrocarbon chain, one can make films with marked layers suitable for measurements of the desorption depth. In such an experiment (Säve et al. 1987a), a target of 13 layers of stearic acid (C) followed by 2 layers of behenic acid (B) and on top of that 2 layers of arachidic acid (A) was constructed, see figure 6. Each layer had a thickness of 25 Å. Analysis of the target with 78 MeV ^{127}I ions showed that the most intense molecular-ion peak was from the bottom layers, indicating a sputtering depth of around 150 Å. The systematic change of the spectra with lower energy density beams excludes the possibility of inhomogenous films and indicates crater formation. The same conclusion was obtained in similar experiments by the Orsay group (Bolbach et al. 1987) and also recently by the Erlangen group (Schmidt et al. 1991b).

To get an idea of the radius of the crater one can use the damage cross section measurements for 78 MeV ^{127}I ions on arachidic acid (Sundqvist et al. 1989). That radius is 80 Å which means that a rather large crater is formed in the case of ^{127}I ions if one assumes that the damage radius is close in size to a removal radius. The number of molecules sputtered from this volume is of the same order of magnitude as the neutral yield obtained for leucine described above. Both Bolbach et al. (1987) and Schmidt et al. (1991b) have developed crater models where the shape of the craters for different beams is discussed. Della-Negra et al. (1990) have measured the dependence of the yield from Langmuir-Blodgett films on the charge state and the angle of incidence of the primary ion. One result from that study is that the strong dependence of the charge state for normal angle of incidence vanishes for grazing angles in agreement with the assumption of a large interaction depth. The general trend in the data can be reproduced with a modified version of the shock wave model (Bitensky & Parilis, 1987).

When using the information obtained from Langmuir-Blodgett experiments one should keep in mind that the oriented Langmuir-Blodgett films could be a rather special case where the film structure promotes sputtering from deep layers and formation of ions from layers below the surface.

7 Energy and Angular Distributions of Secondary Ions

7.1 Axial-Velocity Measurements

The axial velocity component of a secondary ion refers to the component in the direction of the spectrometer axis. The velocity distribution of this component for a certain ion, or corresponding energy distribution, can be obtained from the shape of the corresponding mass line if the acceleration voltages and distances for a straight time-of-flight spectrometer are known with high accuracy (Fürstenau et al. 1977). Becker & Wien (1986) have developed one method for such measurements based on a double acceleration grid arrangement. Macfarlane et al. (1986) and Widdiyasekera et al. (1988) have developed other methods using one grid. For large molecular ions like insulin (5733 u) and LHRH (1801 u) the energies were found by Widdiyasekera et al. to be 3-4 eV, in qualitative agreement with similar measurements by Macfarlane et al. (1986). For the lightest ions H^+ and H_2^+ the initial energies are typically 10 eV but depend on the sample thickness. These light ions are desorbed close to the impact of the primary ion and experience a repulsive force due to the positive charge remaining in the infratrack. This charging effect has also been observed by Macfarlane & Jacobs (1989) when studying H^+ and H_2^+ emission from nitrocellulose films. The 'axial energy' distributions were shifted towards higher values compared to those where the films were covered with an Au layer. Moshammer et al. (1990) have also shown that the positively charged track increases the 'axial energy' for H^+ ions and even reduces it for H^- ions from an organic target compared to a contaminated Au film. An influence of the positively charged track core on the initial radial velocity distributions for H^+ and H^- ions has also been found by Fenyö et al. (1993).

7.2 Radial-Velocity Measurements

The radial velocity component of a secondary ion refers to the component perpendicular to the spectrometer axis. The corresponding velocity distribution can be measured by changing the voltage over a set of deflection plates in the field-free region in a straight time-of-flight spectrometer and measuring the corresponding secondary ion yield, see insert in figure 7. The first experiment of this type was reported by Ens et al. (1989), using fission fragments from a ^{252}Cf source at normal incidence on an insulin target. This experiment gave the surprising result that there is a minimum in the molecular ion yield in the track direction. This is in contrast to the light fragment ion CH_3^+ which has a symmetric distribution whith its maximum along the normal to the surface, see figure 7.

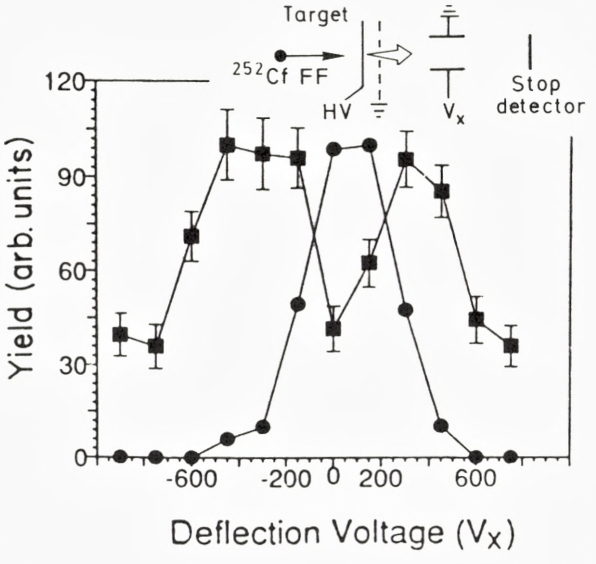

Figure 7. The insert in the figure shows how the radial velocity distribution of secondary ions can be measured in a straight time-of-flight spectrometer. The beam is deflected over the stop detector and the corresponding yield is measured as a function of deflection voltage. The figure shows the result of such a measurement for fission fragments (FF) from a ^{252}Cf source at normal angle of incidence on an insulin target. The fragment ions CH_3^+ (dots) have a distribution around zero deflection voltage corresponding to desorption around the normal to the surface. In contrast to the fragments, the molecular ions of insulin (squares) have an emission minimum in the track direction and are desorbed in a cone out from the target surface. The distributions are normalized to each other, (Ens et al. 1989).

More detailed experiments were performed by Fenyö et al. (1990b) using a small time-of-flight spectrometer that could be rotated around the point of impact of an accelerator beam aimed from behind at a target of renin substrate (1801 u). Results of experiments performed at four different angles are shown in figure 8. The light fragment ions like CH_3^+ have all a symmetric radial velocity distribution around the normal to the target surface, independent of the angle of incidence, and are therefore not shown in the figure. However, the molecular ions of renin substrate have a minimum in the yield with one maximum on each side for perpendicular incidence. When the spectrometer is tilted one of the maxima disappears. Note that for the largest angle (60°) the distribution is closer to ejection along the normal to the surface than for 45° angle of incidence.

The interpretation of the data is that large molecular ions like renin substrate or insulin are ejected at an angle from the surface correlated with the direction

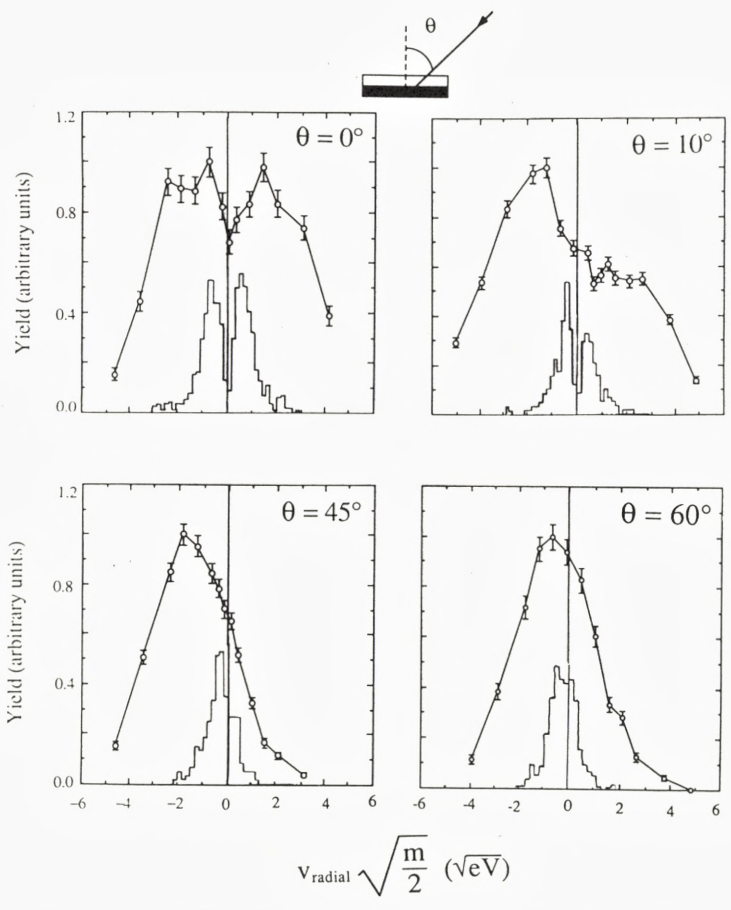

Figure 8. The data points are the measured radial velocity distributions of molecular ions from a renin substrate sample desorbed by 72 MeV ^{127}I ions at four different angles of incidence. The vertical line in each figure denote the centroid of the corresponding distribution for the fragment ion CH_3^+. This ion has the same forward peaked emission pattern independent of the angle of incidence unlike the molecular ions. Compare with figure 7. For each angle of incidence is also shown the corresponding distribution from classical molecular-dynamics simulations of the sputtering event. See text for details, (Sundqvist et al. 1991).

of the incoming primary ion. With the help of the initial axial velocity measurements mentioned above one can estimate an angle of ejection for renin substrate. The results are 43° and 84° with respect to the direction of the primary ion for perpendicular and 45° angle of incidence respectively. These experimental findings strongly support the expansion model by Johnson et al. (1989) and the shock wave model by Bitensky & Parilis (1987) and seem to rule out thermal models in the case of large molecular ion ejection. Both models predict ejection angles of 45° and 67.5° for the two cases in qualitative agreement with the experimental findings. One should however keep in mind that the measurements are for secondary ions and the calculations in the models are for neutral molecules ejected from the surface layer.

The lower curves in figure 8 show the results of classical molecular-dynamics simulations of the sputtering event. The simulations are described elsewhere (Fenyö et al. 1990c; Fenyö & Johnson, 1992) but in brief the basic idea is the following: At time zero a certain number of molecules around the track of the primary ion starts to expand due to e.g. a Coulomb explosion. A Lennard Jones potential is assumed for the interaction between the molecules. By solving the equation of motion for each molecule in time steps, ejection is obtained of molecules. These have a radial velocity distribution in qualitative agreement with the experimental data. One possible explanation for the lack of quantitative agreement in figure 8 between molecular-dynamics simulations and experiment could be that intact ions only leave from adsorbed surface sites (Fenyö 1991).

7.3 Angular-Distribution Measurements

The Darmstadt group has developed a sophisticated position-sensitive stop detector for angular and energy measurements of secondary ions. For each secondary ion the time-of-flight and the position of impact in the detector plane are recorded. The radial and axial velocities as well as the emission angle can then be calculated (Moshammer et al. 1990). Figure 9 shows such measurements by Moshammer (1991) for fission fragments from a ^{252}Cf source at normal incidence on a valine and an alpha-cyclodextrine target respectively. For the latter case an emission minimum for a large negative molecular ion is also demonstrated which rules out the possibility that the emission pattern is caused by the positively charged nuclear track. The same conclusion was also drawn by Fenyö et al. (1990a) who found the same value on the radial velocity component for negative, positive, and also doubly charged molecular ions of bovine insulin desorbed by 72 MeV ^{127}I ions at 45° angle of incidence.

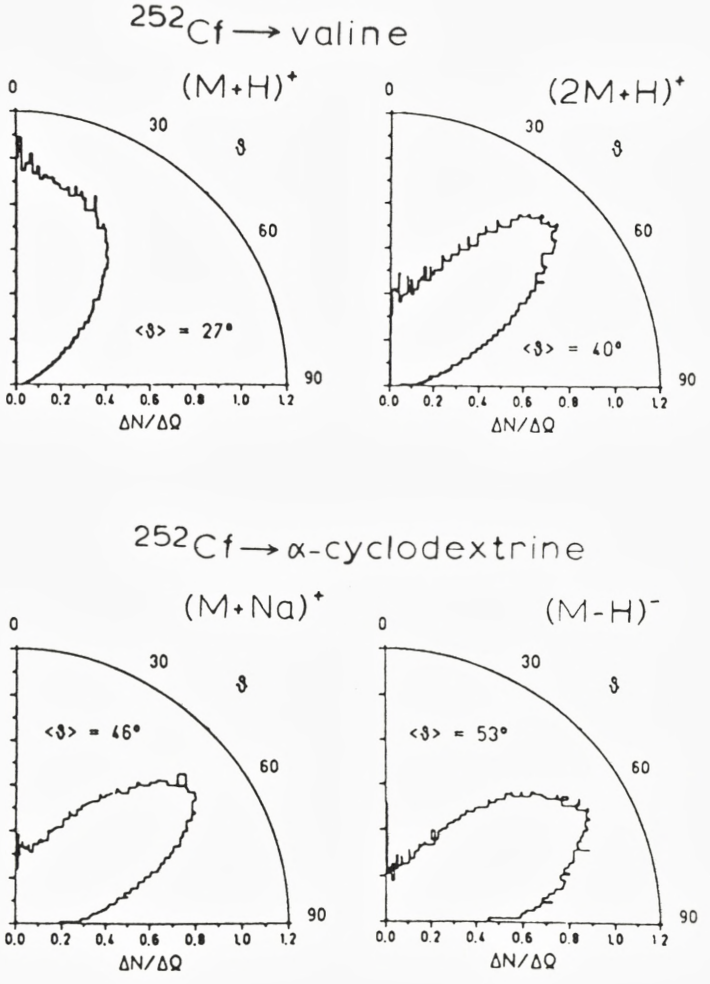

Figure 9. Polar diagrams of angular distributions measured with a position sensitive stop detector of molecular ions from targets of valine and α-cyclodextrine desorbed by fission fragments from a ^{252}Cf source at normal angle of incidence. The molecular ion of valine, $(M+H)^+$, has a forward peaked distribution almost like a $\cos\theta$ distribution unlike the dimer of valine, $(2M+H)^+$, which has an emission minimum in the track direction. In the case of a-cyclodextrine such a minimum is found both for the positive quasi molecular ion, $(M+Na)^+$ and the negative molecular ion, $(M-H)^-$. The latter observation rules out the possibility that the emission pattern is caused by the positively charged ion track. Compare with figure 7 and 8, (Moshammer, 1991).

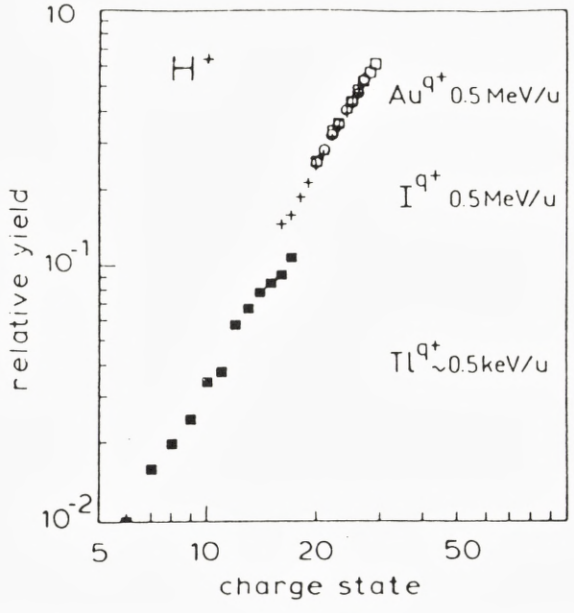

Figure 10. The H^+ yield as a function of the incident charge states of ^{127}I and ^{197}Au ions at 0.5 MeV/u. The yield scales approximately as the incident charge state to the third power. The target is a carbon foil and the H^+ ions have been shown to come from surface contaminants of water and hydrocarbons. The fact that the yield only depends on the incident primary-ion charge state and not on atomic number for constant ion velocity is in marked contrast to what is found for other secondary ions. This indicates that the H^+ emission takes place promptly close to the point of impact of the primary ion. Under the same experimental conditions it has also been found that the H^+ yield for slow heavy ions, ^{208}Tl ions at 0.5 keV/u, scales approximately as the charge state to the third power, (Benguerba et al. 1991b).

8 Emission of Hydrogen Ions

8.1 Hydrogen Emission Induced by MeV Ions

In general, the secondary ion yield in electronic sputtering depends strongly on the charge state (Håkansson et al. 1981a; Becker et al. 1986b; Della-Negra et al. 1987a) and the atomic number of the primary ion (Håkansson & Sundqvist, 1982; Becker et al. 1986a). The yield data have been analyzed in terms of the charge exchange cycle between the primary ion and the solid down to around 100-200 Å. From a description of this cycle it appears that the yield depends on the integrated deposited energy down to that depth (Wien et al. 1987). For the emission of H^+ ions the situation is, however, completely different. Della-Negra et al. (1987c) have shown that, for constant projectile velocity, the yield of H^+ ions from a carbon foil

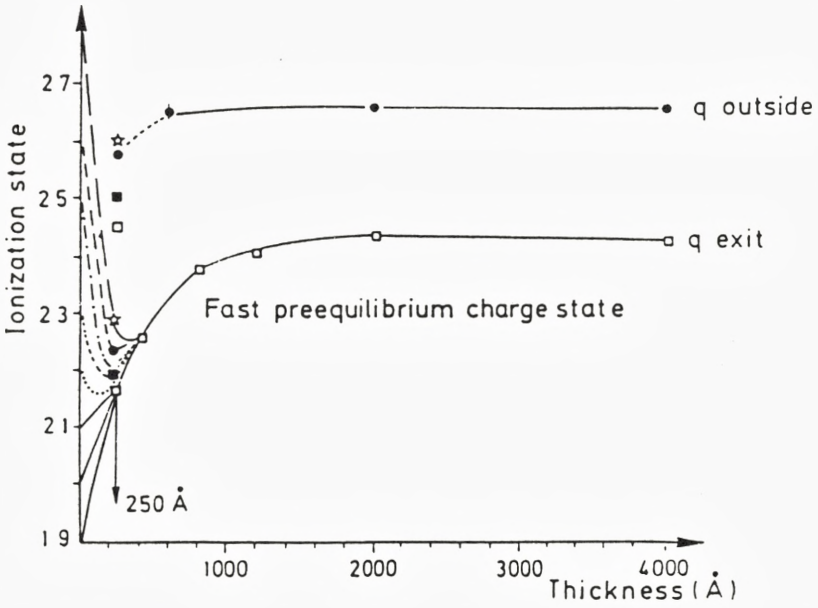

Figure 11. By using the experimental fact that the H^+ yield only depends on the charge state of the heavy ion when it crosses the surface (see figure 10) of the target, the ionization state of the ion inside the foil can be determined. The figure shows the variation of the ionization state of 127 MeV ^{127}I ions as a function of the thickness of different carbon foils traversed. Independent of the incident charge state the ions first reach a preequilibrium charge state which is lower than the final equilibrated charge state (curve (q exit)). This charge state is in turn lower than the charge state obtained 40 ns after the ions have left the foil due to postionization Auger effects (curve 'q outside'), (Benguerba et al. 1991a).

depends only on the primary ion charge when it crosses the surface and not on the atomic number of the primary ion. One such experiment (Benguerba et al. 1991b) was performed employing 0.5 MeV/u ^{197}Au ions ($22 < q < 29$) and ^{127}I ions ($15 < q < 27$). The yield of H^+ ions was found to have almost a cubic dependence on the charge state, independent of the type of ion as shown in figure 10. The emitted H^+ ions were shown to originate from surface contaminants of water and hydrocarbons. The hydrogen emission is thus not dependent on the total energy loss in the foil but rather on the high-energy density deposition in the surface close to the point of impact at an early stage of the energy dissipation.

8.2 Hydrogen Emission Induced by keV Ions

The Orsay group (Benguerba et al. 1991b) has also found the same, almost cubic, charge state dependence for H^+ emission from a carbon foil bombarded with 0.5 keV/u ^{208}Tl ions ($5 < q < 18$) obtained from a radioactive source as shown in figure 10. In this energy range no other ions exhibit a charge-state dependence, not even H^- (Brunelle et al. 1989a). One possible explanation for the emission is that the highly charged primary ion sets up a strong electric field that causes electron emission from the surface before the impact of the ion. The H^+ emission is assumed to be a secondary effect of the electron emission (Della-Negra et al. 1988).

8.3 The Concept of Preequilibrium Charge State

The charge-state dependence of H^+ emission can also be used to determine the mean charge of fast heavy ions inside a foil (Benguerba et al. 1991a). Figure 11 shows the result of such a measurement. Carbon foils of thicknesses between 250 Å and 4000 Å were bombarded with ^{127}I ions at 1 MeV/u. First a calibration curve was established by measuring the H^+ yield from the front side as a function of the charge state. Then the spectrometer was rotated and by measuring the H^+ yield at the exit surface, and by use of the calibration curve the charge state could be determined of the ions just when they left the surface. The finding is that independent of the initial charge state the ions quickly, already at 250 Å, reach a 'preequilibrium charge state'. The full equilibration is reached for much larger film thicknesses and this charge state is found to be lower than the equilibrated charge state measured 40 ns after the ions have left the surface due to postionization Auger effects (Brunelle et al. 1989b).

9 Electronic Sputtering of Small Secondary Ions

For sputtering of intact large biomolecules where a clear nonsymmetric angular distribution has been established, any kind of diffusive model must be excluded. That is however not the case for the fragment ions probably emanating from the hot zone close to the track, the so called infratrack where direct primary ionizations and excitations take place. Moshammer (1991) assumes that from this region, a gaseous flow of particles comes out in the direction of the track. With a simple gas-dynamic model, very good fits can be performed to measured energy and angular distributions. Figure 12 shows such distributions for a positive fragment ion (30 u) of valine ejected for bombardment at normal incidence with a beam of ^{134}Xe ions at 1.4 MeV/u. The gas temperature in this case is 9400 K, and the flow velocity

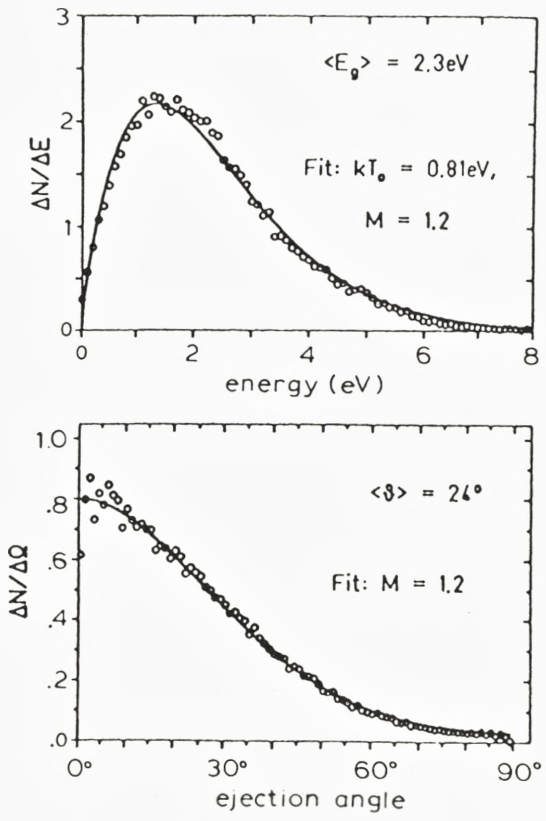

Figure 12. Total energy distribution (upper curve) and angular distribution (lower curve) of a fragment ion (30 u) of valine desorbed by a 1.4 MeV/u ^{134}Xe beam at normal angle of incidence. The fragment ions are believed to be created in the hot central part of the ion track and to be evaporated from the target surface due to a thermal process. The solid lines are calculated in a gas-flow model with the fitting parameters being T_0, the gas temperature and M, the gas flow velocity. In the figure T_0 corresponds to 9400 K and M to 1.2 times the velocity of sound, (Moshammer, 1991).

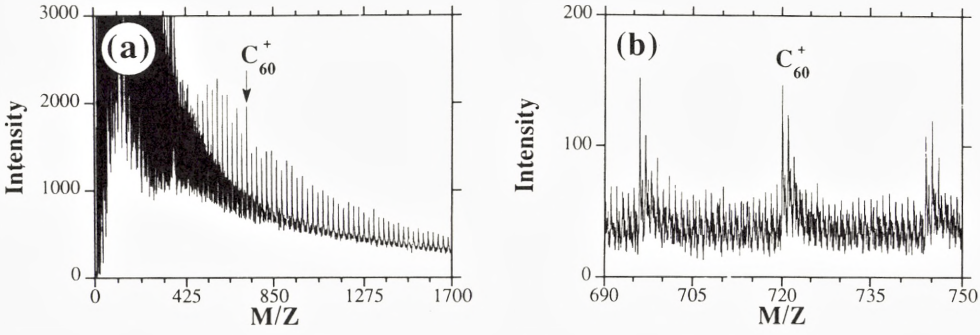

Figure 13. a) When the polymer PVDF, poly(vinylidene difluoride), is irradiated with fast heavy ions even numbered carbon clusters C_n, fullerenes, are promptly formed in the ion track. The figure shows a time-of-flight spectrum of such positive ions with $40 < n < 138$ desorbed by 72 MeV ^{127}I ions. There is an intensity enhancement for the C_{60}^+ (buckyball) ion. b) Expanded view of the region around the C_{60}^+ ion peak from the same spectrum. Due to the ^{13}C isotope each fullerene ion peak splits into several. There is also a peak at every integer mass unit corresponding to different combinations of hydrogenated carbon clusters, (Brinkmalm et al. 1992a).

is 1.2 times the velocity of sound.

However, in the measurements at Uppsala by Fenyö et al. (1990b) of the radial velocity distributions for different angles of incidence of low-mass fragment ions, no indications have been obtained so far of a gas 'jet' of particles going in a direction correlated with that of the incoming primary ion. All angular distributions for low-mass fragment ions measured so far are peaked around the normal to the surface independent of the angle of incidence. Of course, this observation does not rule out other types of thermal processes for the desorption of low-mass fragment ions.

10 Formation of Fullerenes in the Ion Track

When the polymer poly(vinylidene difluoride), PVDF $(CH_2 - CF_2)_n$, is irradiated with fast heavy ions, even-numbered carbon cluster ions are formed (Feld et al. 1990; Brinkmalm et al. 1992a). As shown by Brinkmalm et al. the ions are formed promptly as a consequence of single ion impact, and there is an intensity enhancement for the famous C_{60}^+ (buckyball) ion (Kroto et al. 1985). Arguments that the clusters really consist of only carbon are the systematic trend in the intensity variation of the ^{13}C isotope peaks in the spectra and the accurate determination of their masses. Figure 13 shows a spectrum of positive ions from a PVDF target bombarded with 72 MeV ^{127}I ions. The spectrum is recorded in a time-of-flight spectrometer, see figure 2, equipped with an electrostatic mirror. The latter is

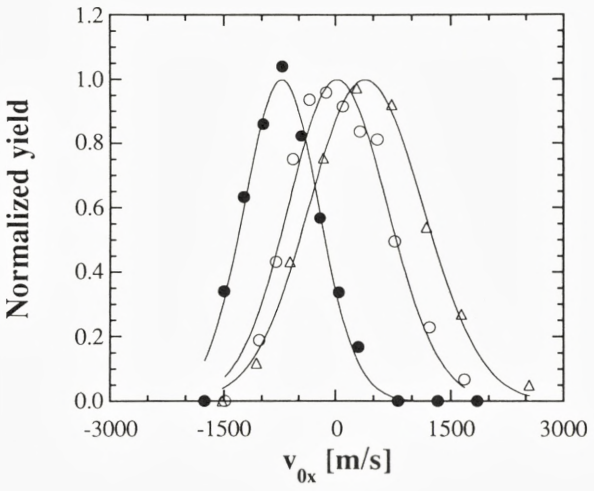

Figure 14. Radial velocity distributions for molecular ions from leu-enkephaline (left curve), C_{60}^+ ions from a synthetic fullerene sample (central curve) and C_{60}^+ ions from a PVDF target (right curve) when bombarded with 72 MeV ^{127}I ions at 45° angle of incidence. The distributions are peak-normalized to the distribution of $C_2H_3^+$ ions which are desorbed symmetrically around the normal to the surface in each case. With respect to the primary ion direction the distributions correspond to ejection angles $> 45°$ for leu-enkephaline, 45° (i.e. ejection normal to the surface) for C_{60}^+ ions from a synthetic fullerene sample and $< 45°$ for C_{60}^+ ions from a PVDF sample. The last case is indicating that the fullerenes are formed in the hot central part of the ion track and ejected due to the axially expanding track, (Brinkmalm et al. 1993).

necessary to use in order to resolve the cluster ions due to extensive metastable decays and, presumably, a broad initial axial velocity distribution of the cluster ions. The clusters are separated by 24 mass units and the pattern extends up to about mass 4000 u. The spectrum also contains peaks at every integer mass unit indicating many combinations of hydrogenated carbon clusters. However, no mixed fluorohydrocarbon ions can be seen in the spectra. From the nearly symmetric peak shapes of the cluster ion peaks one might rule out the possibility that the clusters are formed as decay products of a fullerene precursor that cools down by evaporation in the acceleration region in the spectrometer. It should be noted that no carbon clusters have been observed under irradiation of teflon $(CF_2\text{-}CF_2)_n$ or graphite (which is a conductor) under the same experimental conditions.

The ion-induced fullerene formation is a new phenomenon observed in the field of electronic sputtering of organic molecules. On a very short time scale a considerable atomization occurs followed by mixing and condensation of atoms, leading to the ejection of new molecules completely different from the target material. The

C-C bond is so energetically favoured that the target material locally collapses. The volume occupied by 60 carbon atoms in a vibrationally relaxed C_{60} molecule is eight times smaller than in the original target material (Johnson & Sundqvist, 1992). As will be shown below, there are experiments indicating that this formation takes place in the hot central part of the ion track, a region that so far only has been assumed to eject fragment and atomic ions.

Figure 14 shows a summary of three different measurements of initial radial velocity distributions (Brinkmalm et al. 1993). The peptide leu-enkephalin (555 u), synthetic fullerenes made according to the recipe by Krätschmer et al. (1990) and a film of PVDF were bombarded by 72 MeV ^{127}I ions at 45° angle of incidence. In the figure, the distributions are peak-normalized to the low-mass fragment ion $C_2H_3^+$ which is ejected normal to the surface. The shift of the distribution for molecular ions from leu-enkephalin (left curve) corresponds to an ejection angle larger than 45° away from the direction of the incoming primary ion. This is believed to be a consequence of the radially expanding track as was earlier discussed for other peptides. The distribution for C_{60}^+ ions from the synthetic fullerene sample (central curve) shows no shift compared to the low-mass fragment ion indicating ejection normal to the surface. However, the distribution for the C_{60}^+ ions from the PVDF target (right curve) is shifted in such a way that the ions are desorbed in a direction between the normal to the surface and the direction of the incoming primary ion. This is the first time ejection has been observed in a 'backward' direction, and it is an indication that the fullerenes are formed in the hot central part of the track and that they are desorbed into vacuum from the axially expanding track.

11 Conclusions

To summarize, we have the following picture of an electronic sputtering event in a bioorganic material (compare with figure 3). The fast heavy ion deposits energy along its trajectory in the sample through ionizations and electronic excitations. Light ions like H^+ and H_2^+ are promptly desorbed from regions close to the point of impact at an early stage of the energy dissipation. The emission of these secondary ions serves as a probe of the track before it starts to expand. In the central part of the track the energy density is very high, causing extensive fragmentation of the molecules. These fragments are probably evaporated away from the surface due to some thermal process. As the track starts to expand, a pressure pulse is created that propagates radially and sputters the large molecular ions or neutrals when intersecting the surface with a strong directional correlation. It is supposed that the molecular ions come from regions closer to the central part of the track than the neutrals (Johnson & Sundqvist, 1992).

Central experiments like the scaling to the third power of the neutral yield with the electronic stopping power and the directional correlation are roughly explained by the pressure-pulse model (Johnson et al. 1989), the modified shock-wave model (Bitensky et al. 1991) and by the molecular-dynamics simulations (Fenyö et al. 1990c; Fenyö & Johnson, 1992). However, only when the ions are assumed to come from the surface can these models give agreement with the measured radial velocity distributions. One should keep in mind that almost all experimental data are for ions, and only Bitensky et al. (1991) have attempted to include the ionization step in their theoretical model. Unfortunately the neutral-yield scaling measurement of leucine is the only one performed so far, and this experiment should be repeated for other cases.

Although a large body of experimental information is available today there is still a need for more measurements, especially on total neutral-molecule yields and data related to the ionization processes.

The ion-induced fullerene production from a polymer film is an example of a completely new form of electronic sputtering of organic insulators. Extensive atomization/condensation processes take place promptly upon ion bombardment in the hot central part of the ion track. This leads to the formation of new molecules from an area that so far only has been considered creating fragments and atomic ions. The fullerene production seems to probe the hot core of the axialy expanding track. However, to be able to calculate an ejection angle, measurements on the initial axial velocity distributions are needed.

This paper has described some desorption experiments on organic insulators induced by high energy particle beams. These ions have large stopping power values, up to about 1000 eV/Å. However, the discussed electronic sputtering process also scales down to low stopping power values, about 40 eV/Å , (Salehpour et al. 1989). The relative contributions of electronic and nuclear stopping in the keV energy region to the sputtering yield of organics are however not fully understood as discussed in a review article by Ens in this volume.

Acknowledgements

The author acknowledges the support from the Swedish Natural Science Research Council, the Swedish Research Council for Engineering Sciences and valuable comments on the manuscript by B. U. R. Sundqvist, R. E. Johnson and C. T. Reimann.

References

Becker O and Wien K, 1986: Nucl. Instr. Meth. **B16**, 456
Becker O, Della-Negra S, Le Beyec Y and Wien K, 1986a: Nucl. Instr. Meth. **B16**, 321

Becker O, Guither W, Wien K, Della-Negra S and Le Beyec Y, 1986b: Springer Proc. in Physics 9, Springer Verlag, p. 11

Benguerba M, Brunelle A, Della-Negra S, Depauw J, Joret H, Le Beyec Y, Da Silveira E and Maynard G, 1991a: *Methods and Mechanisms for Producing Ions from Large Molecules*, eds. KG Standing and W Ens, Plenum Press, New York, p. 19

Benguerba M, Della-Negra S, Joret H and Le Beyec Y, 1991b: Int. J. Mass Spectrom. Ion Processes **107**, R11

Bitensky IS and Parilis ES, 1987: Nucl. Instr. Meth. **B21**, 26

Bitensky IS, Goldenberg AM and Parilis ES, 1991: *Methods and Mechanisms for Producing Ions from Large Molecules*, eds. KG Standing and W Ens, Plenum Press, New York, p. 83

Bolbach G, Della-Negra S, Deprun C, Le Beyec Y and Standing KG, 1987: Rapid Commun. Mass Spectrom. **1**, 22

Brandl D, Schoppmann Ch, Schmidt R, Nees B, Ostrowski A and Voit H, 1991: Phys. Rev. **B43**, 5253

Brandt W and Ritchie RH, 1974: *Physical Mechanisms in Radiation Biology*, eds. RD Cooper and RD Wood, USEC Technical Inf. Centre, Oak Ridge, Tennessee, p. 20

Brinkmalm G, Barofsky D, Demirev P, Fenyö D, Håkansson P, Johnson RE, Reimann CT and Sundqvist BUR, 1992a: Chem. Phys. Lett. **191**, 345

Brinkmalm G, Håkansson P, Kjellberg J, Demirev P, Sundqvist BUR and Ens W, 1992b: Int. J. Mass Spectrom. Ion Processes **114**, 183

Brinkmalm G, Demirev P, Fenyö D, Håkansson P, Kopniczky J and Sundqvist BUR, 1993: Phys. Rev. B **47**, 7560

Brunelle A, Della-Negra S, Depauw J, Joret H and Le Beyec Y, 1989a: Nucl. Instr. Meth. **B43**, 586

Brunelle A, Della-Negra S, Depauw J, Joret H, Le Beyec Y and Wien K, 1989b: Nucl. Instr. Meth. **B43**, 484

Brunelle A, Della-Negra S, Depauw J, Joret H and Le Beyec Y, 1991: Rapid. Commun. Mass Spectrom. **5**, 40

Cheblukov YN, Koshkarev DG, Peuto AR, Rudskoygh IV, Vasiliev NA, Nazarov VM, Bock R, Hoffmann DHH, Müller RW and Vetter J, 1992: Particle Accelerators **37/38**, 351

Della-Negra S, Le Beyec Y and Håkansson P, 1985: Nucl. Instr. Meth. **B9**, 103

Della-Negra S, Becker O, Cotter R, Le Beyec Y, Monart B, Standing K and Wien K, 1987a: J. Physique **48**, 261

Della-Negra S, Deprun C and Le Beyec Y, 1987b: Rapid. Commun. Mass Spectrom. **1**,10

Della-Negra S, Le Beyec Y, Monart B, Standing K and Wien K, 1987c: Phys. Rev. Lett. **58**, 17

Della-Negra S, Depauw J, Joret H, Le Beyec Y and Schweikert EA, 1988: Phys. Rev. Lett. **60**, 948

Della-Negra S, Depauw J, Joret H, Le Beyec Y, Bitensky IS, Bolbach G, Galera R and Wien K, 1990: Nucl. Instr. Meth. **B52**, 121

Dück P, Treu W, Fröhlich H, Galster W and Voit H, 1980: Surf. Sci. **95**, 603

Ens W, 1993: Mat. Fys. Medd. Dan. Vid. Selsk. **43**, 155

Ens W, Sundqvist BUR, Håkansson P, Hedin A and Jonsson G, 1989: Phys. Rev. **B39**, 763

Feld H, Zurmühlen R, Leute A and Benninghoven A, 1990: J. Phys. Chem. **94**, 4595

Fenyö D, 1991: Thesis at the Faculty of Science, no 321, Uppsala University, Uppsala, Sweden

Fenyö D and Johnson RE, 1992: Phys. Rev. **B46**, 5090

Fenyö D, Hedin A, Håkansson P, Johnson RE, and Sundqvist BUR, 1990a: *Ion Formation from Organic Solids (IFOS V)*, eds. A Hedin, BUR Sundqvist and A Benninghoven, J. Wiley & Sons, p. 33

Fenyö D, Hedin A, Håkansson P and Sundqvist BUR, 1990b: Int. J. Mass Spectrom. Ion Processes **100**, 63

Fenyö D, Sundqvist BUR, Karlsson BR and Johnson RE, 1990c: Phys. Rev. **B42**, 1895
Fenyö D, Håkansson P and Sundqvist BUR, 1993: Nucl. Instr. Meth. B, in press
Fürstenau N, Knippelberg W, Krueger FR, Weiss G and Wien K, 1977: Z. Naturforsch. **32A**, 711
Haff PK, 1976: Appl. Phys. Lett. **29**, 473
Hedin A, Håkansson P, Sundqvist B and Johnson RE, 1985: Phys. Rev. **B31**, 1780
Hedin A, Håkansson P, Salehpour M and Sundqvist BUR, 1987a: Phys. Rev. **B35**, 7377
Hedin A, Håkansson P and Sundqvist BUR, 1987b: Nucl. Instr. Meth. **B22**, 491
Håkansson P and Sundqvist B, 1982: Rad. Eff. **61**, 179
Håkansson P, Jayasinghe E, Johansson A, Kamensky I and Sundqvist B, 1981a: Phys. Rev. Lett. **47**, 1227
Håkansson P, Johansson A, Kamensky I, Sundqvist B, Fohlman J and Peterson P, 1981b: IEEE Trans. Nucl. Sci. **NS-28**, 1776
Håkansson P, Kamensky I, Salehpour M, Sundqvist B and Widdiyasekera S, 1984: Rad. Eff. **80**, 141
Johnson RE, 1987: Int. J. Mass Spectrom. Ion Processes **78**, 357
Johnson RE and Sundqvist B, 1983: Int. J. Mass Spectrom. Ion Phys. **53**, 337
Johnson RE and Sundqvist BUR, 1992: Physics Today, **March**, 28
Johnson RE, Sundqvist BUR, Hedin A and Fenyö D, 1989: Phys. Rev. **B40**, 49
Jonsson G, Hedin A, Håkansson P, Sundqvist BUR, Säve G, Nielsen P, Roepstorff P, Johansson KE, Kamensky I and Lindberg M, 1986: Anal. Chem. **58**, 1084
Jonsson G, Hedin A, Håkansson P, Sundqvist BUR, Bennich H and Roepstorff P, 1989: Rapid Commun. Mass Spectrom. **3**, 190
Kobetich EJ and Katz R, 1968: Phys. Rev. **170**, 391 and 405
Kraft G, Kraemer M, Scholz M, 1992: Rad. Environ. Biophys. **31**, 161
Kroto HW, Heath JR, Brien SCO, Curl RF and Smalley RE, 1985: Nature **318**, 162
Krätschmer W, Lamb LD, Fostiropoulos K and Huffman DR, 1990: Science **347**, 354
Le Beyec Y, 1989: *Advances in Mass Spectrometry*, Volume 11A, ed. P Longevialle Heyden & Sons Ltd., p. 126
Macfarlane RD and Jacobs DL, 1989: *Ion Formation from Organic Solids (IFOS IV)* , ed. A Benninghoven, J. Wiley & Sons, p. 71
Macfarlane RD and Torgerson DF, 1976: Int. J. Mass Spectrom. Ion Phys. **21**, 81
Macfarlane RD, Hill JC, Jacobs DL and Phelps RG, 1986: *Mass Spectrometry in the Analysis of Large Molecules*, ed. CJ McNeal, J. Wiley & Sons, p. 1
Mamyrin BA, Karataev VI, Shmikk DV and Zagulin VA, 1973: Sov. Phys.-JETP **37**, 45
Matthäus R, Moshammer R, v Hayn G, Wien K, Della Negra S, and Le Beyec Y, 1993: Int. J. Mass Spectrom. Ion Proc. **126**, 45
McNeal CJ, Macfarlane RD and Thurston EL, 1979: Anal. Chem. **51**, 2036
Moshammer R, 1991: Thesis, Institut für Kernphysik, Techn. Hochschule Darmstadt, Germany
Moshammer R, Matthäus R, Wien K and Bolbach G, 1990: *Ion Formation from Organic Solids (IFOS V)*, eds. A Hedin, BUR Sundqvist and A Benninghoven, J. Wiley & Sons, p. 17
Nees B, 1988: Thesis, Physikalisches Institut der Universität Erlangen-Nürnberg, Germany
Qiu Y, Griffith JE, Meng WJ and Tombrello TA, 1983: Radiat. Eff. **70**, 231
Reimann, CT: Mat. Fys. Medd. Dan. Vid. Selsk. **43**, 351
Roepstorff P, 1990: *Mass Spectrometry of Peptides*, ed. DM Desiderio CRC - press, Boca Raton, p. 65
Salehpour M, Håkansson P, Sundqvist B and Widdiyasekera S, 1986: Nucl. Instr. Meth. **B13**, 278
Salehpour M, Hunt JE, Fishel DL and Tou JC, 1989: Int. J. Mass. Spectrom. Ion Processes **88**, 211

Schmidt R, Brandl D, Schoppmann CH, Voit H, Kröhl T, Johannsmann D and Knoll W, 1990: Int. J. Mass Spectrom. Ion Processes **99**, 223

Schmidt R, Nees B, Schoppmann CH, Brandl D, Ostrowski A, Voit H, Johannsmann D and Knoll W, 1991a: Thin Solid Films **195**, 307

Schmidt R, Schoppmann CH, Brandl D, Ostrowski A, Voit H, Johannsmann D and Knoll W, 1991b: Phys. Rev. **B44**, 560

Sigmund P, 1969: Phys Rev **184**, 383

Sundqvist BUR, 1991: *Sputtering by Particle Bombardment, part III*, eds. R Behrisch and K Wittmaack, Springer Verlag, p. 257

Sundqvist BUR, 1993: Int. J. Mass Spect. Ion Proc. **126**, 1

Sundqvist BUR and Macfarlane RD, 1985: Mass Spectrom. Rev. **4**, 421

Sundqvist BUR, Ariyaratne A, Ens W, Fenyö D, Hedin A, Håkansson P, Jonsson G and Widdiyasekera S, 1989: *Ion Formation from Organic Solids (IFOS IV)*, ed. A Benninghoven, J. Wiley & Sons, p. 51

Sundqvist BUR, Håkansson P, Hedin A, Fenyö D, Brinkmalm G, Roepstorff P and Johnson RE, 1991: *Methods and Mechanisms for Producing Ions from Large Molecules* eds. KG Standing and W Ens, Plenum Press, New York, p. 7

Säve G, Håkansson P, Sundqvist BUR, Johnson RE, Söderström E, Lindqvist SE and Berg J, 1987a: Appl. Phys. Lett. **51**, 1379

Säve G, Håkansson P, Sundqvist BUR, Söderström E, Lindqvist S-E and Berg J, 1987b: Int. J. Mass Spectrom. Ion Processes **78**, 259

Tang X, Beavis R, Ens W, LaFortune F, Schueler B and Standing KG, 1988: Int. J. Mass Spectrom. Ion Processes **85**, 43

Torgerson DF, Skowronski RP and Macfarlane RD, 1974: Biochem. Biophys. Res. Com. **60**, 616

Voit H, Nieschler E, Nees B, Schmidt R, Schoppmann CH, Beining P and Scheer J, 1989: J. de Physique **C2**, 237

Walter K, Boesl U and Schlag EW, 1986: Int. J. Mass Spectrom. Ion Processes **71**, 309

Watson CC and Tombrello TA, 1985: Rad. Eff. **89**, 263

Widdiyasekera S, Håkansson P and Sundqvist BUR, 1988: Nucl. Instr. Meth. **B33**, 836

Wien K, 1989: Rad. Eff. Defects in Solids **109**, 137

Wien K, 1992: Nucl. Instr. Meth. **B65**, 149

Wien K, Becker O, Guthier W, Della-Negra S, Le Beyec Y, Monart B, Standing KG, Maynard G and Deutsch C, 1987: Int. J. Mass Spectrom. Ion Processes **78**, 273

Williams P and Sundqvist B, 1987: Phys. Rev. Lett. **58**, 1031